340
5-16-80

Dr. 1490

DOE/ET/23002-T3

POLYACETYLENE, $(CH)_x$, AS AN EMERGING MATERIAL FOR SOLAR CELL APPLICATIONS

Second Quarterly Technical Progress Report, July–September 1979

By
A. J. Heeger
A. G. MacDiarmid

MASTER

U-63e

Work [illegible]

University of [illegible]
Philadelphia, Penns[illegible]

U.S. Department of Energy

Solar Energy

DISTRIBUTION OF THIS DOCUMENT IS UNLIMITED

DISCLAIMER

Available from the National Technical Information Service, U. S. Department of Commerce, Springfield, Virginia 22161.

Price: Paper Copy $6.00
Microfiche $3.50

DOE/ET/23002-T3
Distribution Category UC-63e

TECHNICAL PROGRESS REPORT
(July, August, September, 1979)
(Second Quarterly Progress Report)

POLYACETYLENE, $(CH)_x$, AS AN EMERGING MATERIAL FOR SOLAR CELL APPLICATIONS

Contract No. DE-AC04-79ET-23002

UNIVERSITY OF PENNSYLVANIA
Philadelphia, Pennsylvania 19104

A. J. Heeger

A. G. MacDiarmid

DISTRIBUTION OF THIS DOCUMENT IS UNLIMITED
RB

Introduction

As of the starting date of this contract, a variety of rectifying junctions had been fabricated using doped and undoped $(CH)_x$. Schottky diodes formed between metallic AsF_5-doped $(CH)_x$ and n-type semiconductors indicate high $[CH(AsF_5)_y]_x$ electronegativity. The p-type character of undoped trans-$(CH)_x$ was confirmed by Schottky barrier formation with low work function metals. An undoped p-$(CH)_x$:n-ZnS heterojunction solar cell has been demonstrated by our group with open circuit photovoltage of 0.8 V. These results point to the potential of $(CH)_x$ as a photosensitive material for use in solar cell applications.

The devices fabricated in initial experiments fall into three categories: 1) Schottky diodes utilizing heavily doped $(CH)_x$ as a metallic electrode on a variety of n-type semiconductors, 2) Schottky diodes utilizing undoped $(CH)_x$ as a p-type semiconductor on which metallic contacts are placed, and 3) p-n heterojunction diodes formed at the interface of undoped p-type $(CH)_x$ on n-ZnS.

Several n-GaAs:(metallic)$[CH(AsF_5)_y]_x$ diodes were produced by direct polymerization of the $(CH)_x$ film on the semiconductor surface. As indicated by C-V and I-V characteristics, all had barrier heights in the range of 0.8 - 1.0 eV consistent with the results for most metal:GaAs interfaces. Solar cells were fabricated using thin semi-transparent $[CH(AsF_5)_y]_x$ films. Illumination through the polymer with a tungsten lamp produced open circuit photovoltages in the range 0.4 - 0.6 V.

A p-n heterojunction was produced from undoped trans-$(CH)_x$: n-ZnS. Estimates of the actual photoyield (corrected for point contact collector electrode) implied a quantum efficiency for the $(CH)_x$:n-ZnS junction approaching unity at 3.1 eV. This represents photoactivation of carriers in $(CH)_x$ since such a photoresponse from ZnS at a photon energy 0.6 eV below its band gap with light illuminating the junction through $\sim$ 1 mm of ZnS is impossible. Under illumination of approximately 1 sun, an open circuit voltage of 0.8 V was obtained. Short circuit current was limited by series resistance ($\sim 10^9\ \Omega$!!) due to the point contact collector electrode.

During the first quarter of this contract, efforts were directed toward obtaining the necessary equipment; and on probing a variety of different junction configurations. During the second quarter, our efforts have focussed on a particular device configuration for evaluation and study. In particular the p-n heterojunction system, p-$(CH)_x$:n-CdS is being used to evaluate the potential of polyacetylene, $(CH)_x$, as an emerging material for solar cell applications. In parallel with this heterojunction effort, we are studying Schottky junctions made of heavily doped metallic polyacetylene on various inorganic semiconductors. The goal of this second effort is to control the electronegativity of this metallic polymer through variation of the dopant species and dopant concentration. In this way one can hope to achieve larger Schottky barrier heights and hence more efficient Schottky junction solar cells.

Progress During Current Quarter and Plans for Next Quarter

A. Equipment

Controlled Atmosphere Dry Box (Vacuum Atmospheres Corp.
Hawthorne, California)
Including:

- HE-43-2 Dri-Lab, single work station, right end ante chamber
- HE-303 Fluorescent Skylight
- HE-503-1 Shelf Assembly
- HE-213-4 Glove port cover
- 2626-2 Circulation Filter
- HE-03 Dri-Lab Stand
- Electrical measurements input-output
- Associated accessories

The Dry Box is on hand and has been put into operation. Its use simplifies handling procedures and avoids contamination.

Spectrophotometer
Including:

- McPherson monochromator
- Light sources (UV through IR)
- Light chopper/shutter for synchronous detection
- Ithaco Lock-in amplifier
- Gratings and filters cover the working range
- Calibrated detector

Most items have arrived and a working spectrometer (200 nm → 1.2 μ) is available. Installation included fitting components together, construction of a light shield for the beam after it leaves the monochromator, and adjustment of components as needed for our information and for best performance of the system.

Some items remain to be delivered, including IR filters and detector, digital wavelength counter, xenon lamp, and beam handling mirrors. Interfacing to a computer, for full usefulness, has been initiated.

B. p-$(CH)_x$: n-CdS Heterojunctions

Earlier efforts using n-ZnS as the n-substrate for our $(CH)_x$ polymer studies experienced continuing difficulties. ZnS is notoriously difficult to dope and to make ohmic contacts onto in a routine manner. During July considerable progress was made to the point of achieving satisfactory results (contact resistance $\sim$ 30 KΩ, $\rho \sim$ 1000 Ω-cm) on occasional attempts. However, the continuing difficulties caused us to switch to single crystal CdS for the n-type substrate. CdS can be obtained commercially at desired doping levels. Moreover making ohmic contacts to CdS is essentially routine. Our procedure involves wiping In-Sn solder onto a crystal with a cool soldering iron. Total 2-probe resistances of less than 5Ω are now routinely achieved (across crystal of dimensions 1 mm x 5 mm x 3 mm). The CdS single crystal material (n-type, $n = 10^{17}$ cm^{-3}, $\rho \simeq 3 \times 10^{-2}$ Ω-cm at 300 K), was purchased from Eagle-Picher. After x-ray alignment to establish the cleavage planes ([$11\bar{2}0$] and [$10\bar{1}0$]), the large crystal was cut with a diamond coated wire saw. Subsequently pieces were cleaved for our heterojunction experiments with $(CH)_x$.

To summarize, the features of CdS which make it an attractive n-type substrate:

1) Ease of handling

    A) Doping
    B) Ohmic Contacts
    C) Cleaving

2) Electronic properties

    A) Egap = 2.42 eV (ZnS Egap = 3.58 eV) so like ZnS, CdS absorption is small over the solar spectrum.
    B) Electron affinity = 4.5 eV (ZnS Electron affinity = 3.9 eV)

Different electron affinities should yield different built-in potentials in junctions with p-$(CH)_x$. Thus changing substrate materials to vary electron affinity represents a good cross check.

    C) CdS (like ZnS) has the property that on freshly cleaved surfaces, barrier voltages are <u>not</u> determined by surface states (as is the case in Si and GaAs).

The p-$(CH)_x$:n-CdS heterojunction has been studied using a variety of techniques including the following:

1) I vs V

2) $1/c^2$ vs V

3) Photovoltaic spectral response

4) Photovoltaic response time

In addition, we carried out experiments designed to compare the properties of pressure contact junctions to those formed by polymerization directly on CdS substrates.

Crystalline films of polyacetylene were grown in the presence of a Zeigler catalyst (see H. Shirakawa, T. Ito and S. Ikeda, Die Macromolecular Chemie <u>179</u>, 1565 (1978) and references therein). Films were either free-standing or grown directly on the CdS substrate. Routine checks showed that exposure of the CdS crystal to the catalyst caused no harmful effects. For example Au : CdS Schottky diodes were not dependent on previous exposure of the CdS to the catalyst. X-ray diffraction and scanning electron micrograph studies show that the films are polycrystalline and consist of matted fibrils which are typically 200 Å in diameter as shown in the attached electron micrograph. The measured density of the $(CH)_x$ films is 0.4 gm/cm^3 compared with 1.2 gm/cm^3 as obtained by flotation techniques. Thus the volume filling fraction of fibrils is approximately $\frac{1}{3}$. The *cis-trans* content was controlled by thermal isomerization. Samples used in the junction and photovoltaic studies were the thermodynamically stable *trans*-isomer.

i) I-V Data on p-$(CH)_x$: n-CdS Heterojunctions

High quality diodes were obtained with excellent forward/back ratio. Using $(CH)_x$ films of $\sim 100\ \mu$ thickness, forward bias characteristics yielded series resistances, $R_s \sim 10^4\ \Omega$ as shown in Figures 1 and 2 (junction area $\sim 0.1\ cm^2$). A $10\ \mu$ film reduced the series resistance to $R_s \sim 10^3\ \Omega$ (Fig. 3). Thus the R_s of these junctions is being determined by the $(CH)_x$ resistivity. This result is quantitatively accounted for by the known resistivity, $\rho($*trans*$\text{-}(CH)_x) \simeq 10^5\ \Omega\text{-cm}$. Thus, for a 1 cm^3 junction with $(CH)_x$ thickness of $10\ \mu$, we expect $R_s \simeq 10^3\ \Omega$. Since the resistivity of $(CH)_x$ can be decreased by many orders of magnitude we see no major problem in the series resistance parameter. Future work to reduce R_s will utilize

SEM micrographs of $(CH)_x$; the upper panel is as-grown film, the lower panel is oriented film. The typical fibril diameter is 200 Å.

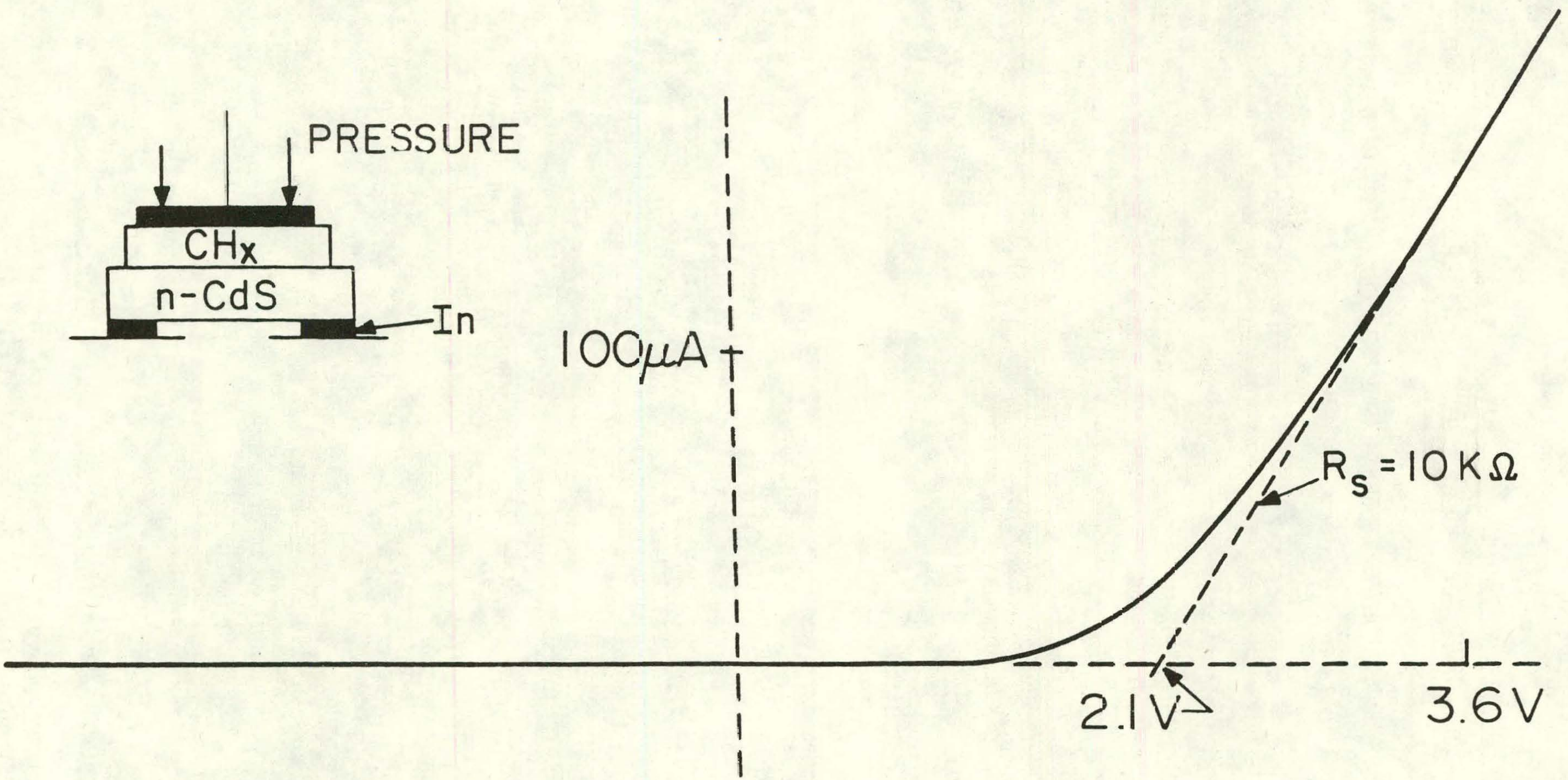

Figure 1

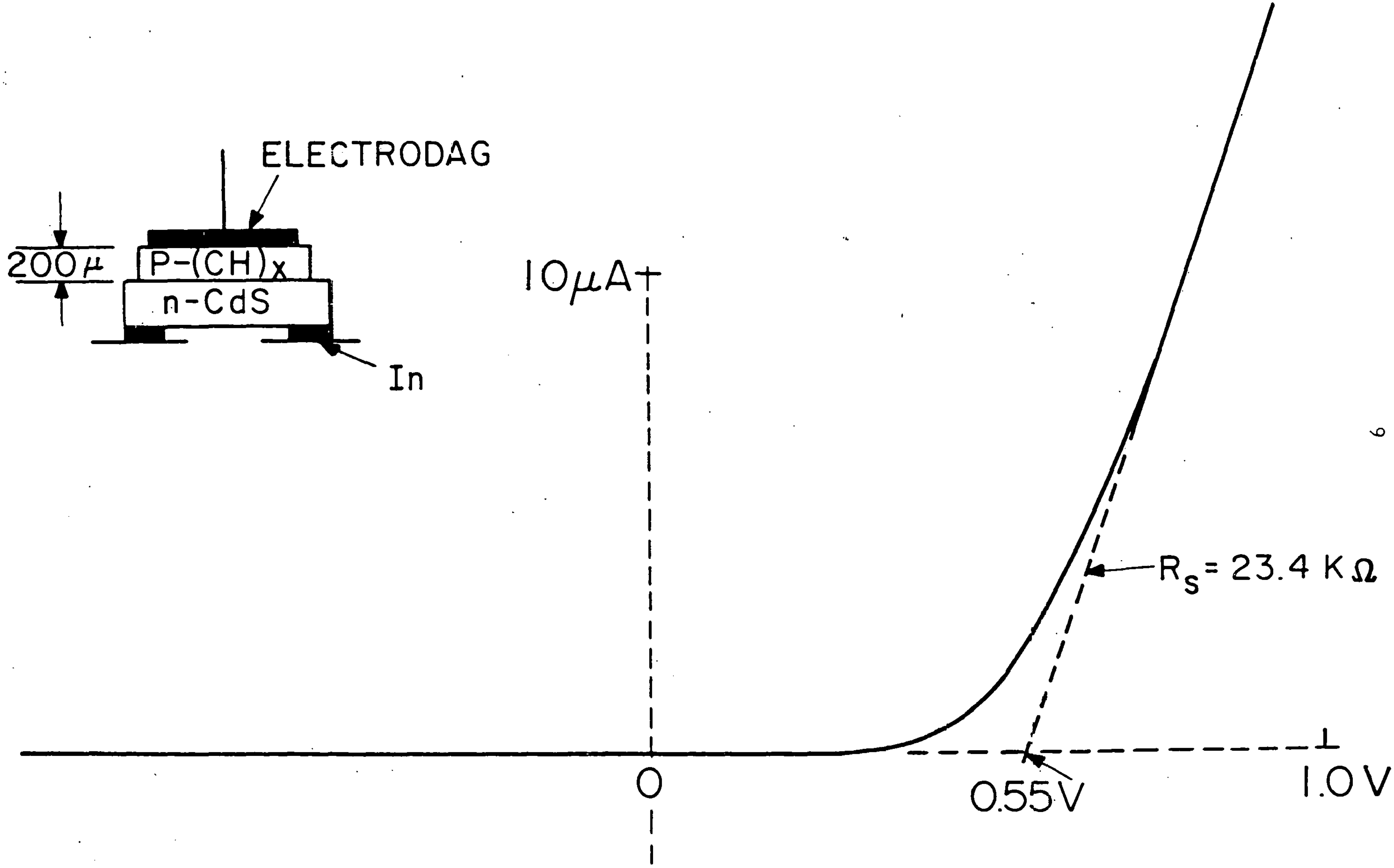

Figure 2

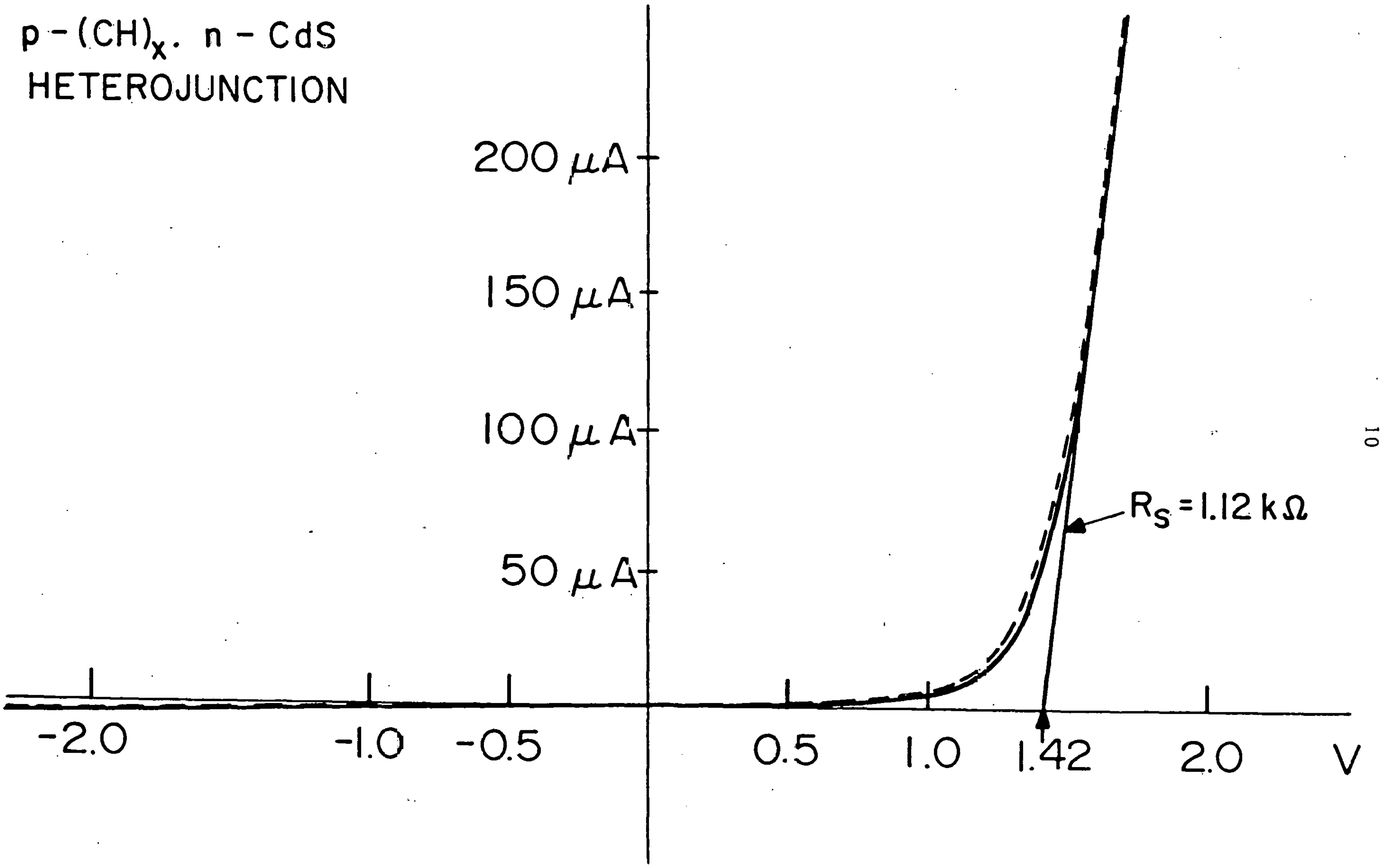
p - (CH)x . n - CdS
HETEROJUNCTION
200 μA
150 μA
100 μA
50 μA
-2.0
-1.0
-0.5
0.5
1.0
1.42
2.0
V
RS = 1.12 kΩ

Figure 3

1) Thinner films

2) Light doping

With these two variables, further reduction in R_s should be readily achievable. For example use of a 1 μ thick film with $\rho = 5 \times 10^4$ Ω-cm (typical of trans-$(CH)_x$) will yield a series resistance of 5 Ω for a 1 cm^2 cross section. Very light subsequent doping should eliminate any series resistance problem.

ii) Photovoltaic Spectral Response of p-$(CH)_x$: n-CdS Heterojunctions

The photovoltaic spectral resonance curves (plotted as relative quantum efficiency vs photon energy) of pressed contact and as-grown junctions are shown in Figures 4 and 5. The results are qualitatively similar to the $(CH)_x$: ZnS heterojunction data and exhibit a frequency dependence similar to that of the photoconductivity of undoped $(CH)_x$ (see Fig. 6). The existence of the shoulder near 1.5 eV (with a steep fall off at lower photon energies) is consistent with a bandgap for $(CH)_x$ of $E_g \sim 1.5$ eV.

As in $(CH)_x$: ZnS junctions, a peak is observed at ~ 0.9 eV (not shown on Figs. 4, 5, and 6), the intensity of which depends on the previous illumination history of the junction. Possible sources of this response peak are: a $(CH)_x$ deep level trap or a conduction band trap due to a band matching spike. Characterization of this low energy peak (origin, decay times, etc.) will be a focus of our efforts in the next quarter (October - December, 1979).

iii) Capacitance Measurements of p-$(CH)_x$: n-CdS Heterojunctions

Plots of $1/c^2$ vs V were linear over a wide bias range as shown

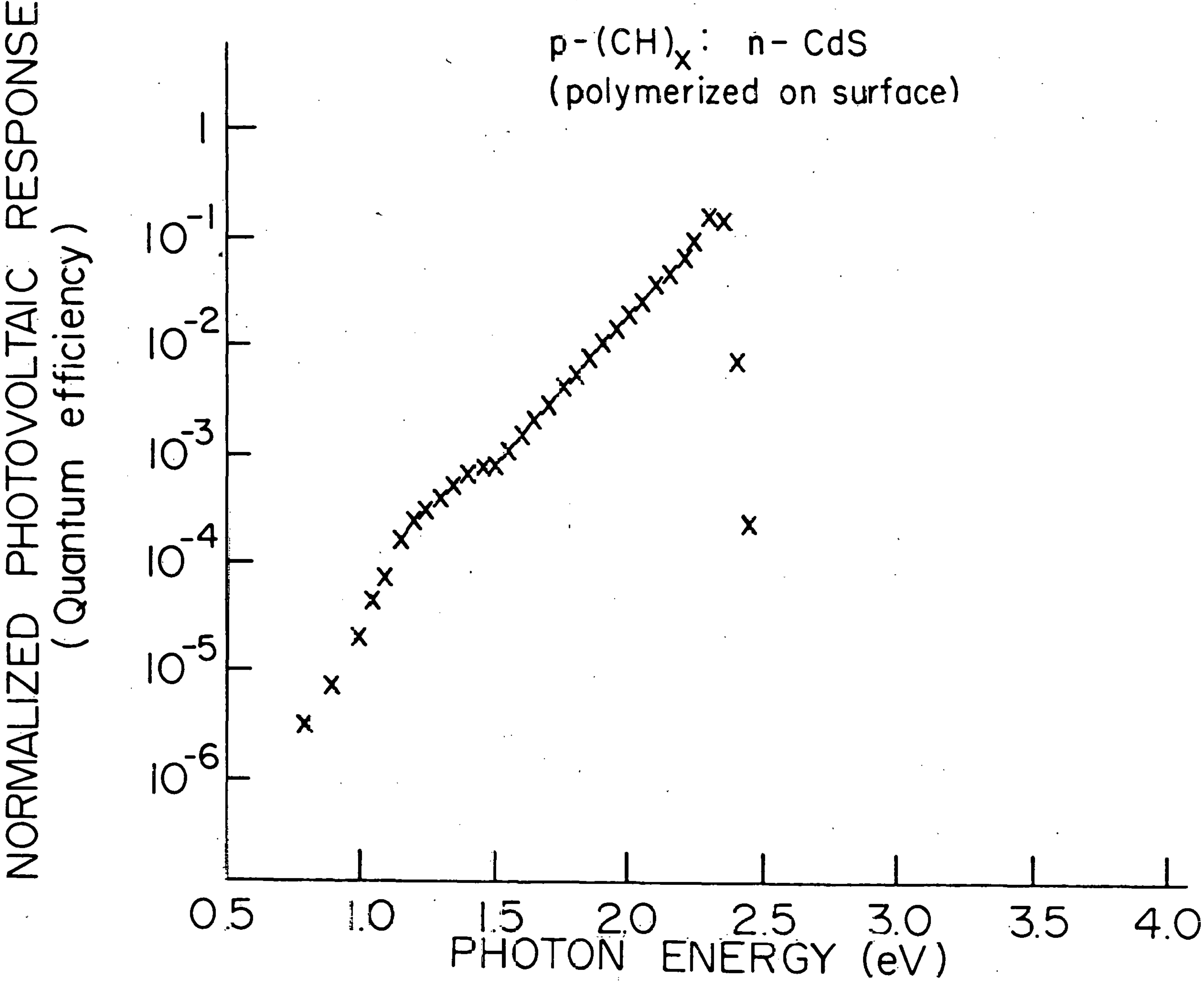
p-(CH)$_x$: n- CdS
(polymerized on surface)
NORMALIZED PHOTOVOLTAIC RESPONSE
(Quantum efficiency)
1
10^{-1}
10^{-2}
10^{-3}
10^{-4}
10^{-5}
10^{-6}
0.5
1.0
1.5
2.0
2.5
3.0
3.5
4.0
PHOTON ENERGY (eV)

Figure 4

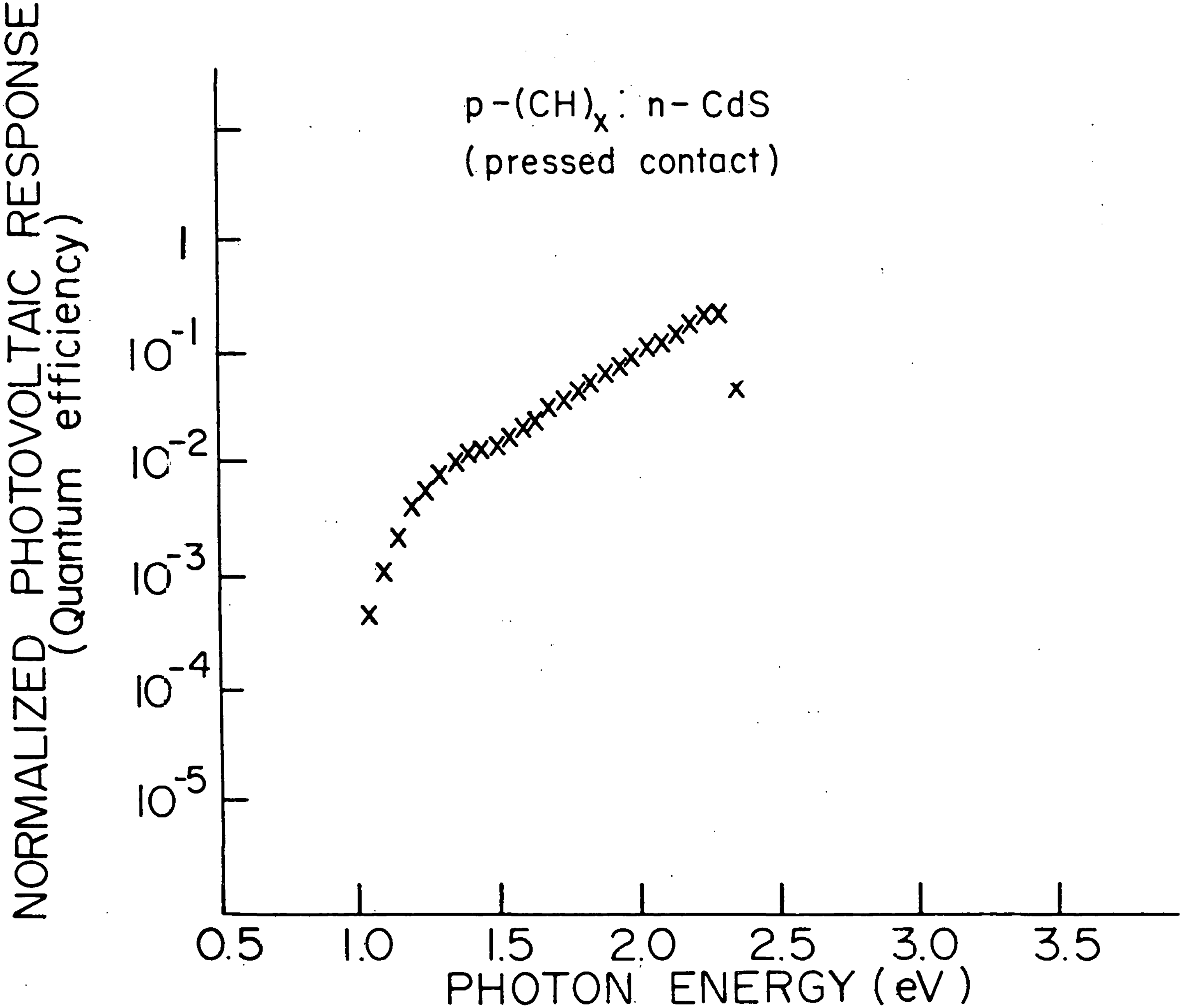
p-(CH)$_x$: n-CdS
(pressed contact)
NORMALIZED PHOTOVOLTAIC RESPONSE
(Quantum efficiency)
1
10^{-1}
10^{-2}
10^{-3}
10^{-4}
10^{-5}
0.5
1.0
1.5
2.0
2.5
3.0
3.5
PHOTON ENERGY (eV)

Figure 5

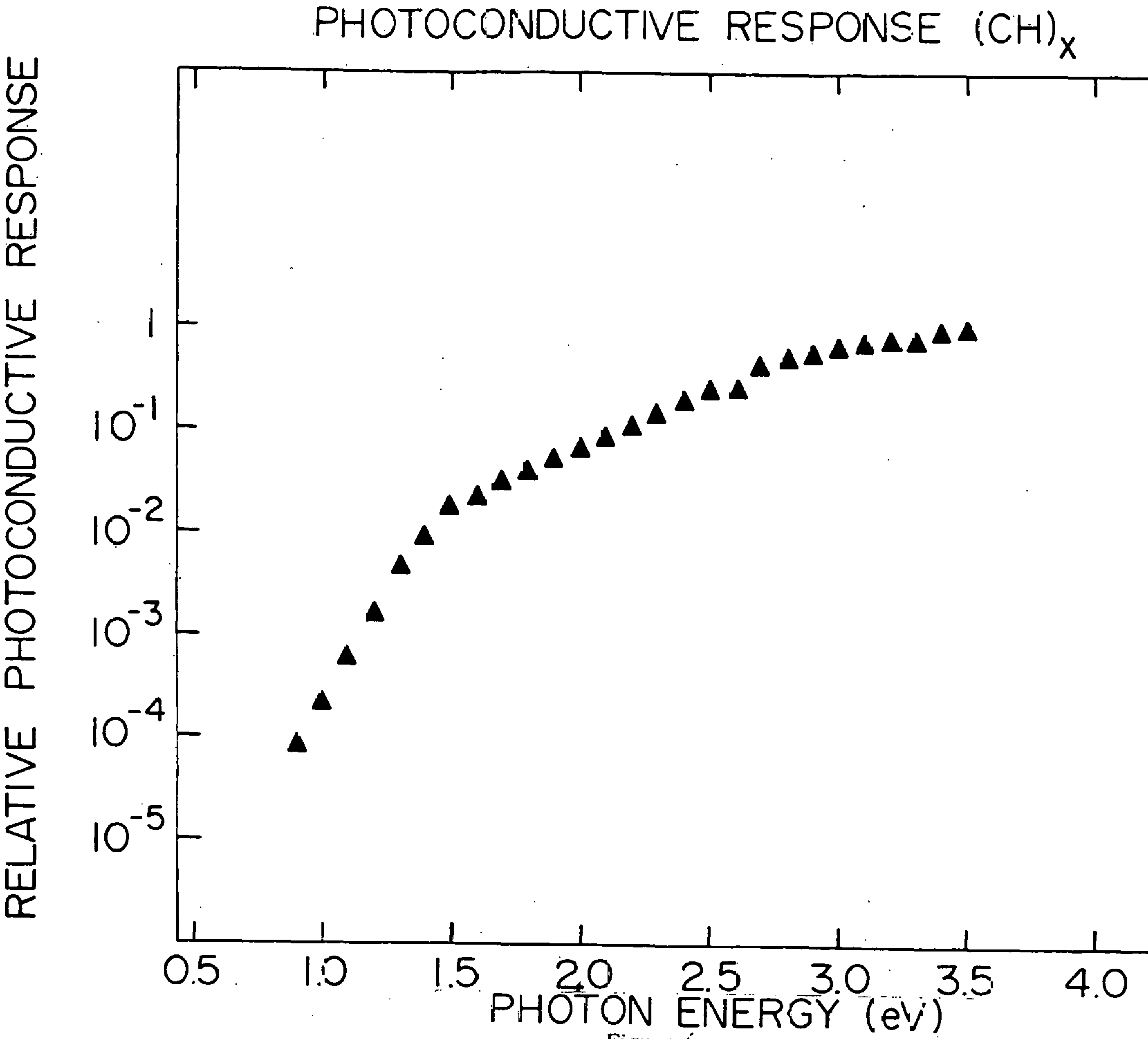
PHOTOCONDUCTIVE RESPONSE $(CH)_x$
RELATIVE PHOTOCONDUCTIVE RESPONSE
1
10^{-1}
10^{-2}
10^{-3}
10^{-4}
10^{-5}
0.5
1.0
1.5
2.0
2.5
3.0
3.5
4.0
PHOTON ENERGY (eV)

Figure 6

in Figures 7 and 8. The voltage intercept generally yielded a built-in potential of approximately 1.9 volts.

To verify the CdS carrier concentration, a Au : CdS Schottky diode was fabricated and data obtained for $1/c^2$ vs V. Analysis yielded n(CdS) = $1.1 \times 10^{17}\ cm^3$ in excellent agreement with the nominal value.

iv) Photovoltaic Response Time of p-$(CH)_x$: n-CdS Heterojunctions

The p-$(CH)_x$: n-CdS junctions represent major progress in this area. Previous measurements on ZnS-$(CH)_x$ heterojunctions indicated a long (~ 15 sec) response time. Work on CdS-$(CH)_x$ heterojunctions indicate that the long response time was not due to a long lived trap in $(CH)_x$ or a heterojunction band matching spike as originally thought. Both pressure contact junctions and as-grown junctions have now been fabricated with CdS for which the photovoltaic response times are less than 0.1 sec. Thus, the response time is not a major problem, nor is it indicative of traps etc. intrinsic to $(CH)_x$.

v) Initial Evaluation of p-$(CH)_x$: n-CdS Heterojunctions

Related studies carried out under separate funding have established that undoped $(CH)_x$ is p-type with $p = 2 \times 10^{18}\ cm^{-3}$. Microwave measurements on oriented $(CH)_x$ indicate that the parallel dielectric constant is $\epsilon_p \simeq 10$ (see C. R. Fincher, Jr., M. Ozaki, A. J. Heeger and A. G. MacDiarmid, Phys. Rev. B 19, 4140 (1979)). Using these values, plus $n = 10^{17}\ cm^{-1}$ and $\epsilon_n = 10$ for CdS, we estimate the width of the depletion layer to be

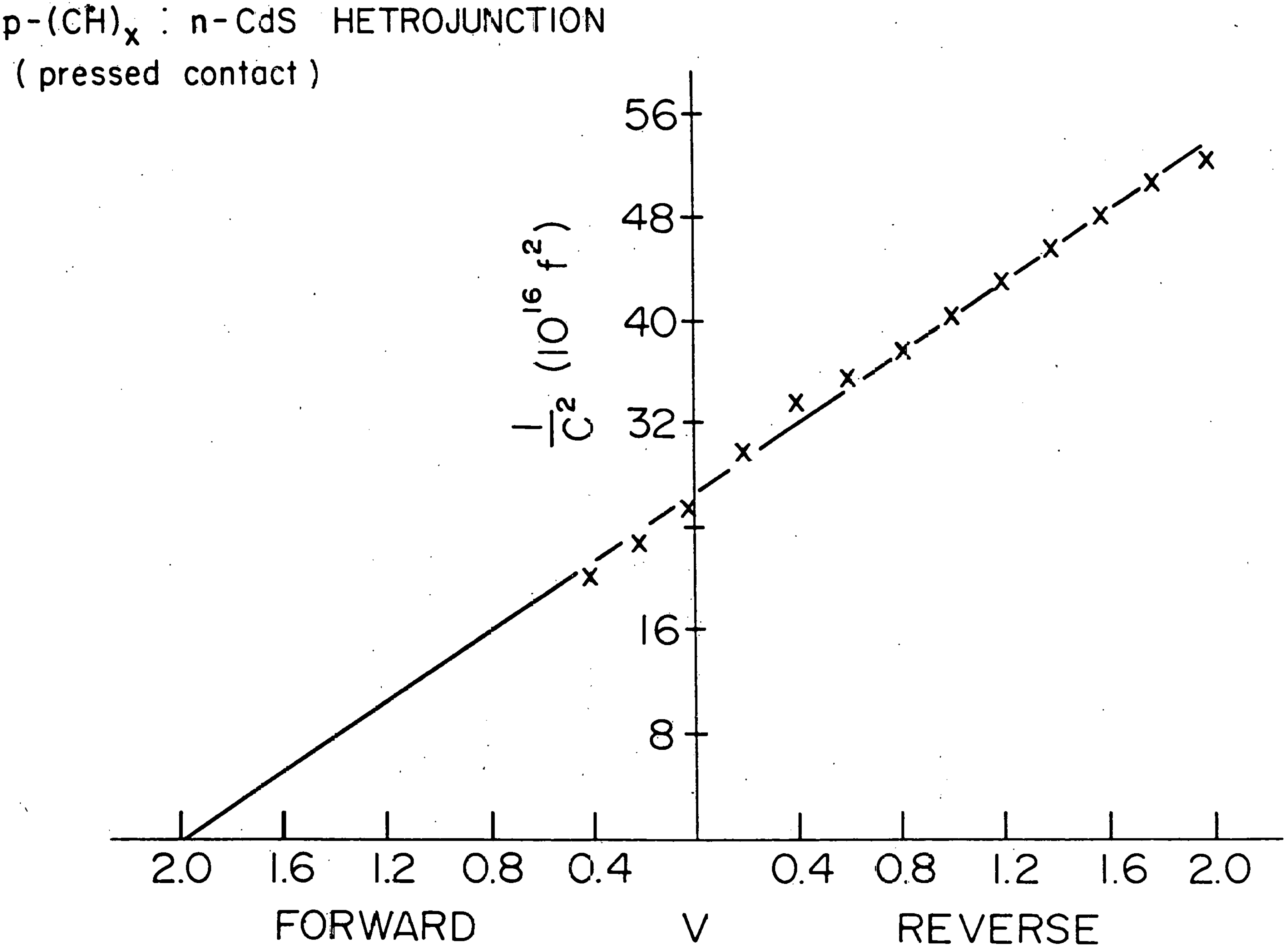
p-(CH)$_x$: n-CdS HETROJUNCTION
(pressed contact)
$\frac{1}{C^2}$ (10^{16} f^2)
56
48
40
32
16
8
2.0
1.6
1.2
0.8
0.4
0.4
0.8
1.2
1.6
2.0
FORWARD
V
REVERSE

Figure 7

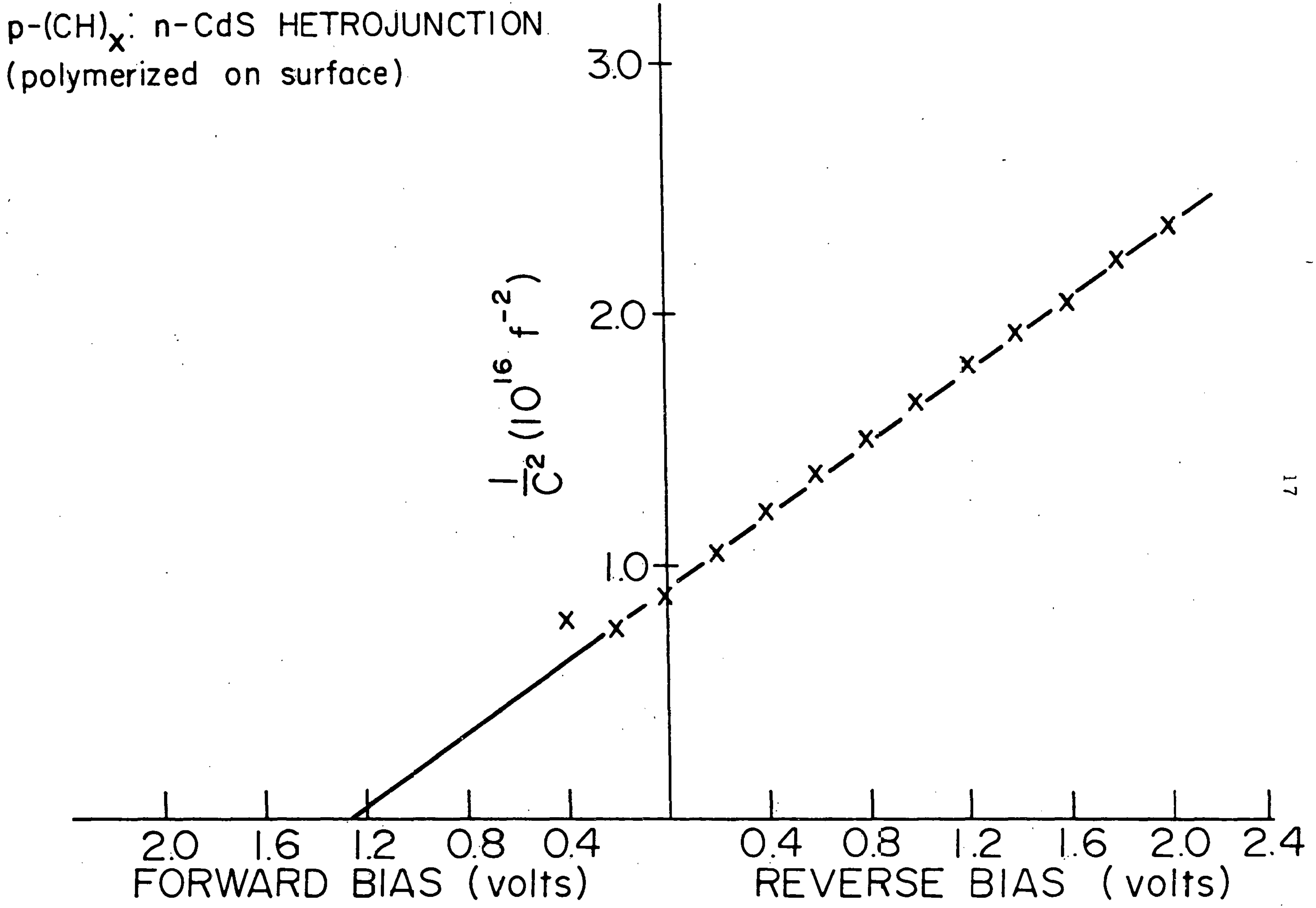
p-(CH)x: n-CdS HETROJUNCTION
(polymerized on surface)
$\frac{1}{C^2}$ (10^{16} f^{-2})
3.0
2.0
1.0
2.0
1.6
1.2
0.8
0.4
0.4
0.8
1.2
1.6
2.0
2.4
FORWARD BIAS (volts)
REVERSE BIAS (volts)

Figure 8

$$W = \left[\frac{2\epsilon_n \varepsilon_p V_{Bi}(N_p + N_n)^2}{q(\epsilon_p N_p + \epsilon_m N_n) N_n N_p}\right]^{\frac{1}{2}}$$

$$\simeq 1400 \text{ Å}$$

Since the depletion layer can be written

$$W = X_n + X_p$$

where X_n and X_p are the widths in the CdS and $(CH)_x$ respectively, we may write

$$\frac{X_p}{X_n} = \frac{N_n}{N_p}$$

$$\simeq 0.05$$

Thus, only 70 Å is depleted in the $(CH)_x$; i. e. less than the width of a single fibril! Since the optical absorption coefficient at 1.5 eV photon energy is $\alpha(1.5) \sim 10^5 \text{ cm}^{-1}$, the carrier collection efficiency is extremely poor. The above analysis treats the polymer as an effective medium and averages over the fibril structure.

In summary, the primitive initial configurations utilized have two major problems:

1) High series resistance

2) Depletion layer almost completely in CdS with resultant carrier collection efficiency very poor.

Neither of these problems is intrinsic to the polyacetylene. Both can in principle be solved by varying the thickness and carrier concentration in the polymer. Since both thickness and carrier concentration are controlled variables in the $(CH)_x$ system, we foresee no fundamental problems.

Plans for the next quarter include initial attempts to correct the above problems and evaluate efficiencies of the fabricated cells.

C. Schottky Diode Photovoltaic Cells Using Metallic $[CH(AsF_5)_y]$

Schottky diodes were fabricated using metallic $[CH(AsF_5)_y]_x$ on n-CdS. In this mode the doped polymer is acting as the electronegative metal in contact with the n-CdS to form a Schottky barrier at the interface. CdS has an advantage over the covalent semiconductors (Si and GaAs) previously used in that the properties of the junctions are sensitive to the electronegativity of the metal rather than being determined solely by surface states.

Initial experiments were carried out by polymerizing a thin film of $(CH)_x$ on a CdS crystal. This was then treated with AsF_5 to dope the $(CH)_x$ to the metallic regime. The samples prepared in this way did not give a good photoresponse, i. e. both the voltage and current generated for a given illumination were very small. This is apparently due to a chemical reaction between CdS and the AsF_5 dopant. Such reactions would harm the active CdS interface in contact with the Doped $(CH)_x$.

Another technique was then developed. The CdS crystal was pressed onto a piece of AsF_5-doped $(CH)_x$ film (*ca.* 0. 1 mm thickness) which was supported by a glass slide. Light was then incident through the CdS to the interface of the CdS and the doped $(CH)_x$. Electrical contact to the $(CH)_x$ film was made by means of an alligator clip. Electrical contact to the CdS was made by melting indium (m. p. 156.6° C) with a soldering iron on the CdS surface and then attaching a copper wire to it. The Schottky barrier so formed acts as a photosensitive diode for light with photon energies less than 2.4 eV. At higher energies, the incident light is absorbed in the CdS.

Figure 9 shows I-V curves for this diode in the dark and under illumination of one sun. The open circuit voltage is about 0.4 V and the short circuit current is about 40 μ Amps/cm^2.

Since the photons incident on the junction all have energy less than the band gap of CdS, the photosensitivity and photovoltaic effect arise from electron photoemission from the metallic $(CH)_x$. Figure 10 shows a plot of the characteristic photoresponse indicative of photoemission: we plot (relative photoresponse)$^{\frac{1}{2}}$ vs photon energy. For photoemission the corresponding plot should be linear with intercept (i. e. onset of response) at an energy equal to the barrier height (V_B). Figure 10 therefore implies $V_B \simeq 0.93$ Volts. The low frequency tail is not understood, but may arise from inhomogeneity in the polymer. An alternative method of determining V_B is from the traditional $1/C^2$ vs V plot shown in Fig. 11. The intercept gives $V_B \simeq 1.2$ V. Differences of this magnitude (i. e. .93 V from

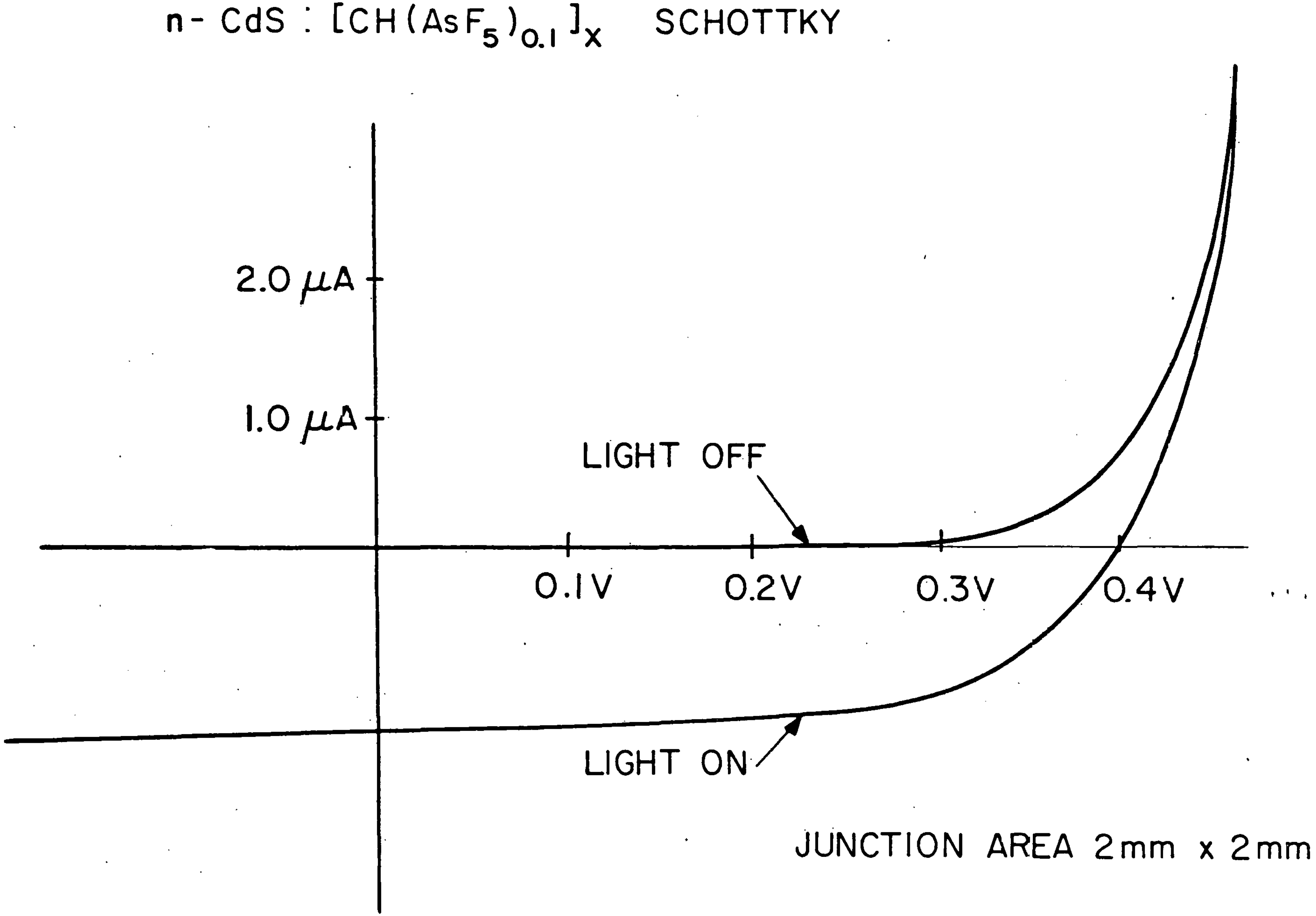
n- CdS : $[CH(AsF_5)_{0.1}]_x$ SCHOTTKY
2.0 μA
1.0 μA
LIGHT OFF
0.1V
0.2V
0.3V
0.4V
LIGHT ON
JUNCTION AREA 2mm x 2mm

Figure 9

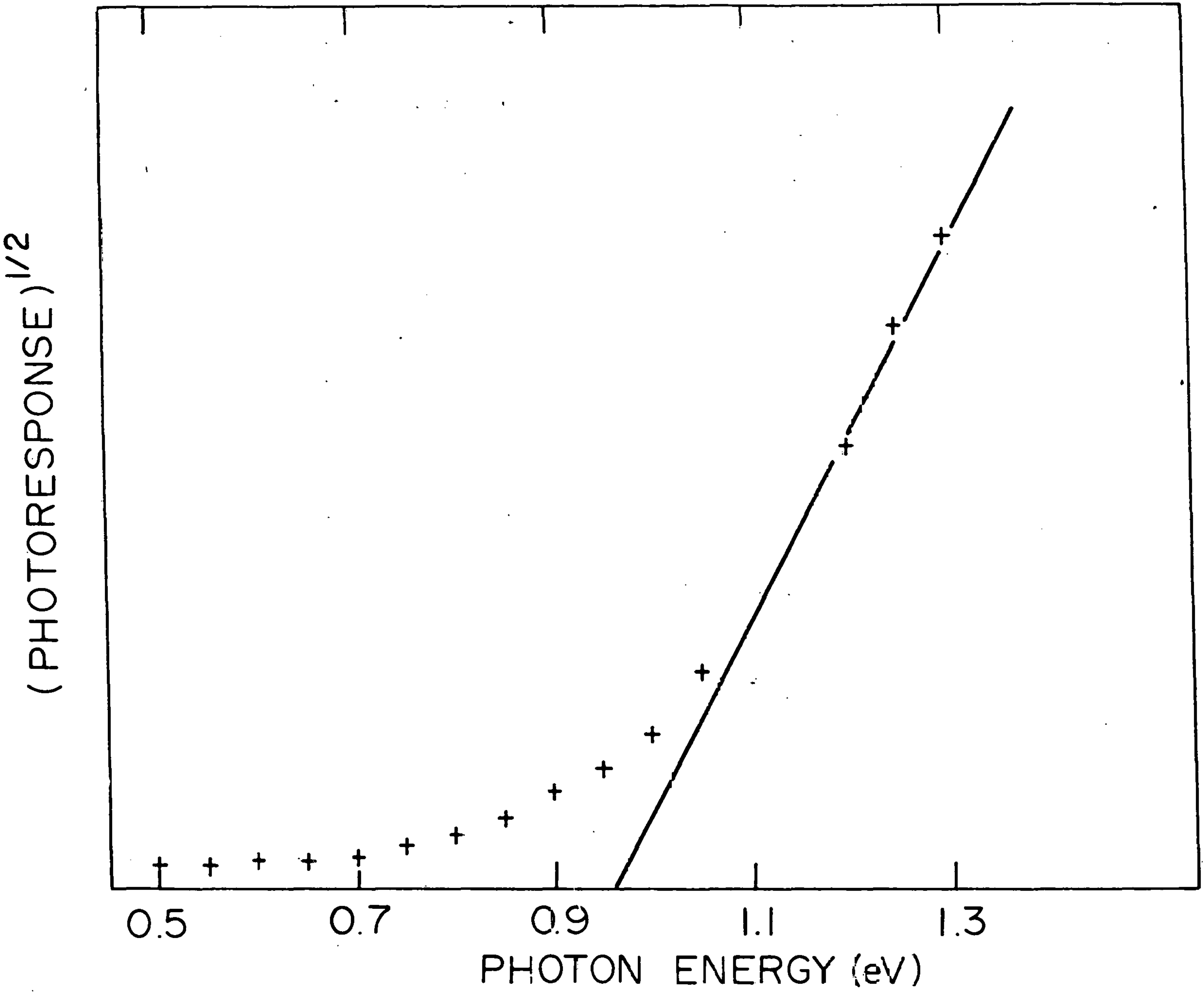

Figure 1C

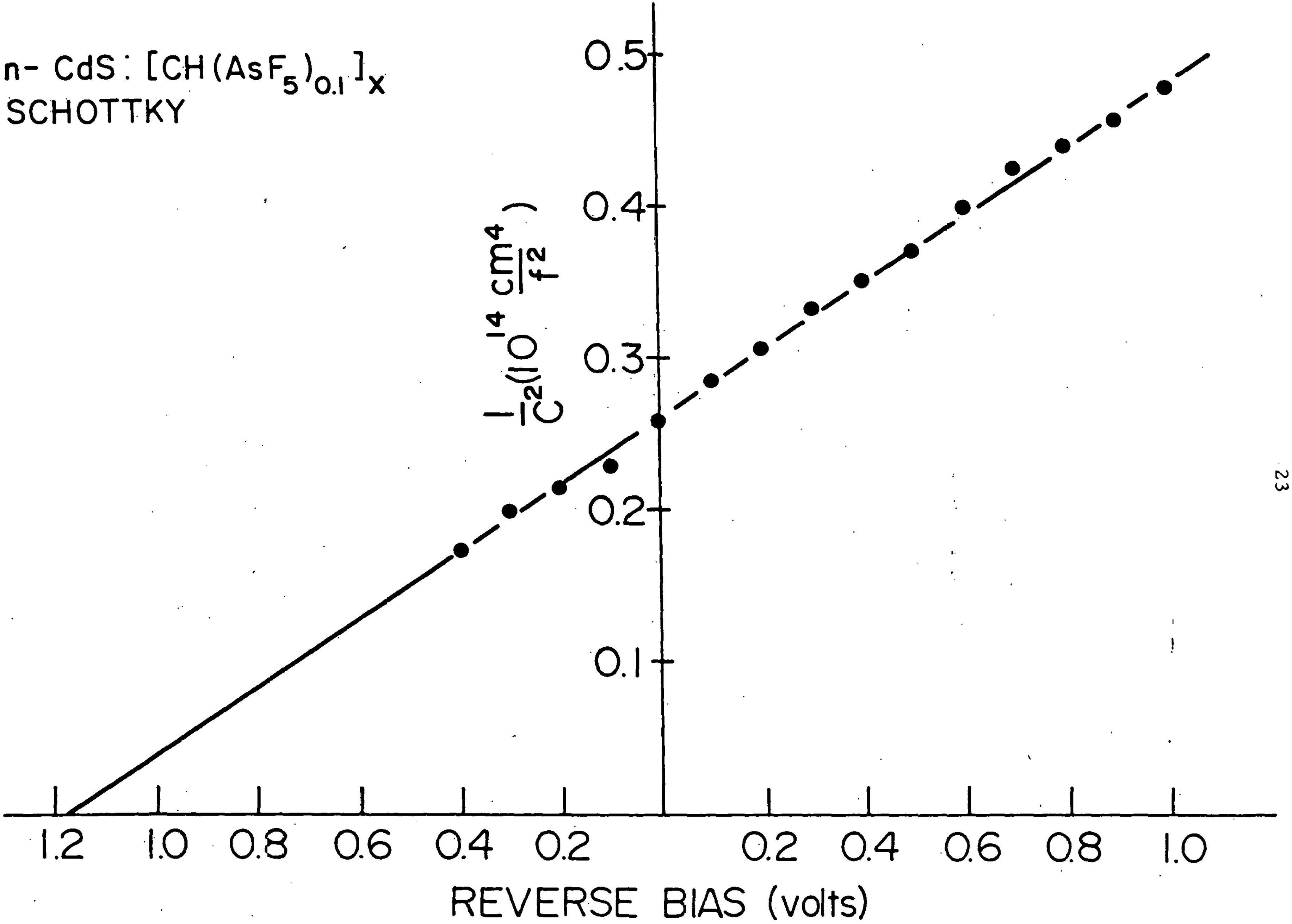
n- CdS : [CH(AsF5)0.1]x
SCHOTTKY
0.5
0.4
0.3
0.2
0.1
1/C² (10¹⁴ cm⁴/f²)
1.2
1.0
0.8
0.6
0.4
0.2
0.2
0.4
0.6
0.8
1.0
REVERSE BIAS (volts)

Figure 11

photoresponse and 1.2 V from C-V) are not unusual. This relatively large barrier height implies a relatively high electronegativity for metallic $[CH(AsF_5)_y]_x$.

Detailed studies, planned for coming months, involve carrying out similar experiments with different dopants in an attempt to control the electronegativity and achieve maximum barrier heights.

October, 1979 ERC41029.2QR

DOPED POLYACETYLENE, CH_x, FOR SOLAR CELL APPLICATIONS

Quarterly Report No. 2
For period 07/01/79 through 09/30/79

Subcontract No. 5-25508-0

General Order No. 41029

Prepared for:

Department of Physics
University of Pennsylvania
Philadelphia, Pennsylvania 19104

Prepared by:

J S Harris

J. S. Harris, Jr.
Program Manager

Rockwell International
Electronics Research Center

THIS PAGE

WAS INTENTIONALLY

LEFT BLANK

During the second quarter of this program, we have concentrated on two areas: (i) the development of Schottky barrier structures for use with polyacetylene, and (ii) the development of an FET structure to use for doping/mobility measurements.

I. $(CH)_x$ Schottky Barriers

One of the stumbling blocks in the way of achieving low cost solar cells through the use of $(CH)_x$ has been the inability to form either stable homojunctions or Schottky barriers. Heterojunctions forfeit much of the cost savings by using conventional semiconductors as the n-half of the junction.

In order to form Schottky barriers to p-$(CH)_x$, a survey of the electropositive metals was begun. The first effort was to compare metal-$(CH)_x$ contacts using Mg ($x = 1.2$ on the Pauling scale) with those using Au ($x = 2.4$). The basic experiment was x-ray photoelectron spectroscopy (XPS) which is illustrated in Fig. 1. The important point is that XPS measures all the energies relative to the Fermi energy.

The samples measured were unintentionally doped (p-type) $(CH)_x$ films deposited on Au plated XPS sample holders. In the first phase of the experiment, half the sample was masked and a ^{1S}C spectrum was taken. A layer of Mg was deposited on the $(CH)_x$ in situ with a thickness that allowed detection of Mg but barely decreased the C signal. This was likely no more than several monolayers. The ^{1S}C spectrum was repeated and found to have shifted by 1 eV towards greater binding energy. This results from the band bending which occurs during p-type Schottky barrier formation and is shown in Fig. 1. A thin layer of gold was then deposited on the Mg and the ^{1S}C line remained shifted, i.e., the subsequent Au layer did not shift the Schottky barrier. The Au was thickened to passivate the Mg, the mask was removed and the experiment was repeated on the other side of the sample using Au rather than Mg. In this case, no shift in the ^{1S}C line was observed (Fig. 2). The implication of these experiments is that gold forms an ohmic contact to $(CH)_x$ and Mg

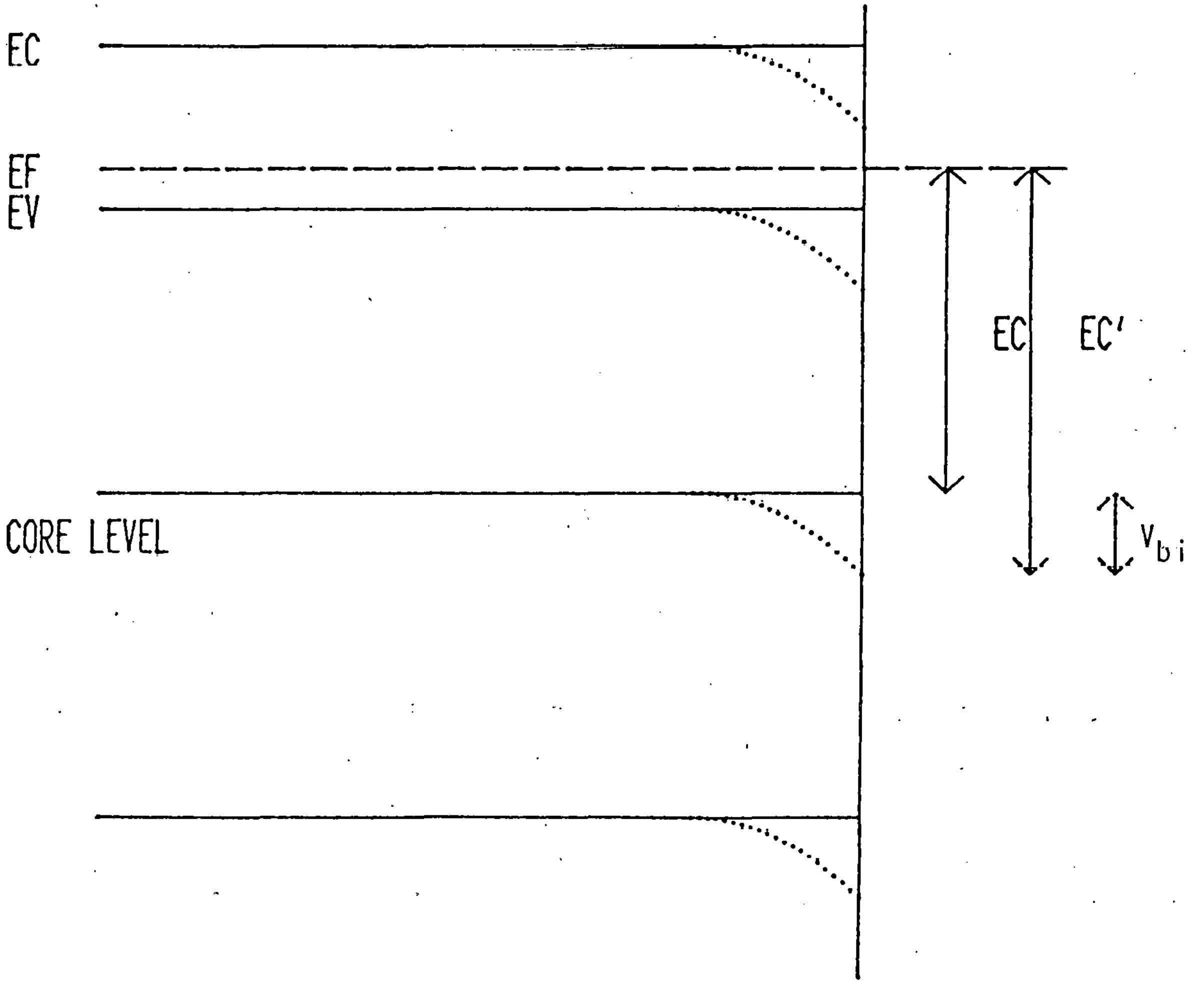

Fig. 1. XPS determination of V_{bi} by measuring shift in core level.

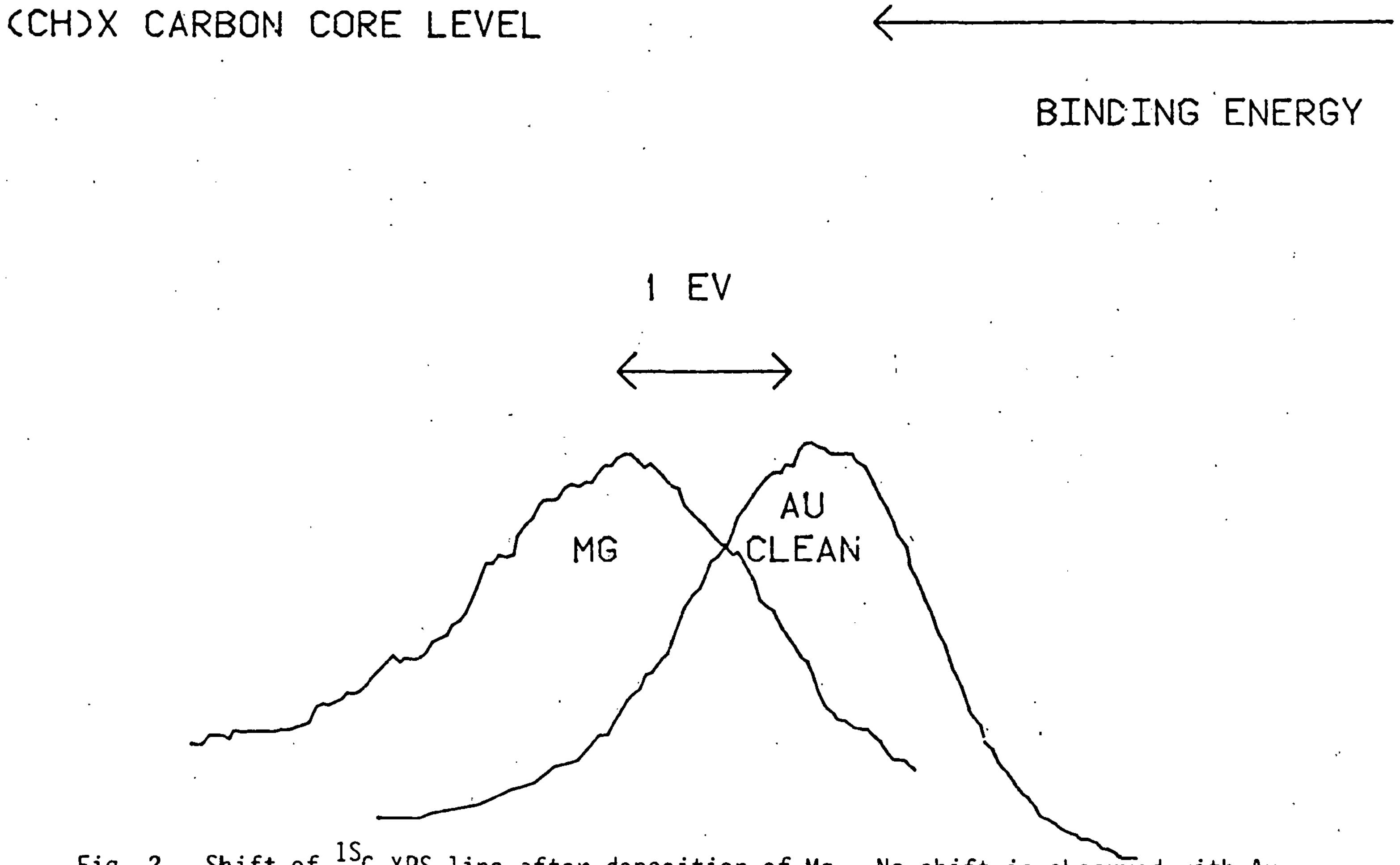

Fig. 2. Shift of ^{1S}C XPS line after deposition of Mg. No shift is observed with Au.

forms a Schottky barrier.

The use of XPS has several advantages including its model independence (unlike I-V, C-V or internal photoemission), its applicability to high resistivity samples and the lack of a need to make electrical contacts. It tends, however, to underestimate barrier heights. The change in core level positions measures the change in built-in potentials resulting from the application of the metal. The presence of surface states would have caused the bands to be bent in the "clean" sample so that the true built-in potential is greater than the measured change. In addition, the barrier height in any p-type semiconductor is greater than the built-in potential by the energy difference between the Fermi level and the valence band maximum (Fig. 1). In unintentionally doped material, this can be considerable.

The exciting result of this experiment, then, is that the Mg:$(CH)_x$ Schottky barrier height appears to be greater than 1 eV.

The samples were removed from the XPS chamber and 250 micron Schottky diodes were isolated photolithographically. The I-V characteristics are shown in Fig. 3. As can be seen, the Au:$(CH)_x$ contacts have symmetric and linear I-V characteristics indicating ohmic behavior while the Mg:$(CH)_x$ contacts exhibit strong p-type rectification. This is clear from the data despite the high bulk resistivity of the undoped $(CH)_x$.

C-V measurements were carried out at 1 KHz with a guard ring structure to minimize edge effects. The in phase and out of phase portions of the admittance were analyzed in terms of series resistance and capacitance and the results for the capacitance are shown in Fig. 4. The parameters extracted are, at best, qualitative due to the severity of the data reduction in this high resistivity sample. The zero bias capacitance ($C/A \sim 3.4 \times 10^{-8}$ F/cm^2) implies a depletion depth ($\epsilon/\epsilon_0 \sim 9$) of $W \cong 2300$Å. With a barrier height of 1 eV, this would occur in material with a doping of $N_A \sim 1.8 \times 10^{16}$ cm^{-3} in qualitative agreement with the 1.3×10^{16} obtained from the slope of the $1/C^2$ vs. V curve. The underestimation of the barrier height from C-V measurements probably results from a combination of the sensitivity of the data reduction algorithm and the possibility of added capacitance due to surface states.

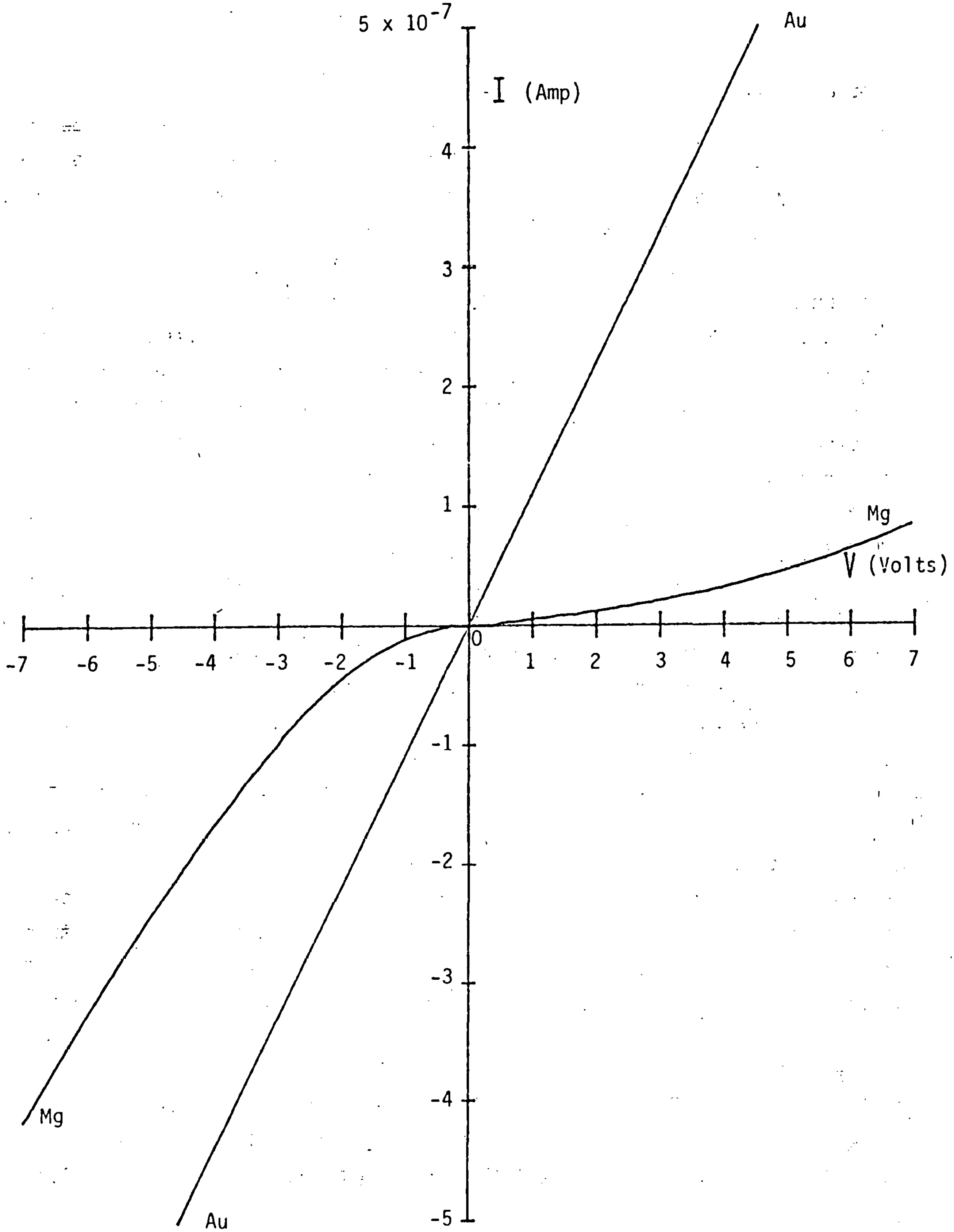

Fig. 3. I-V characteristics of Au:$(CH)_x$ and Mg:$(CH)_x$ contacts.

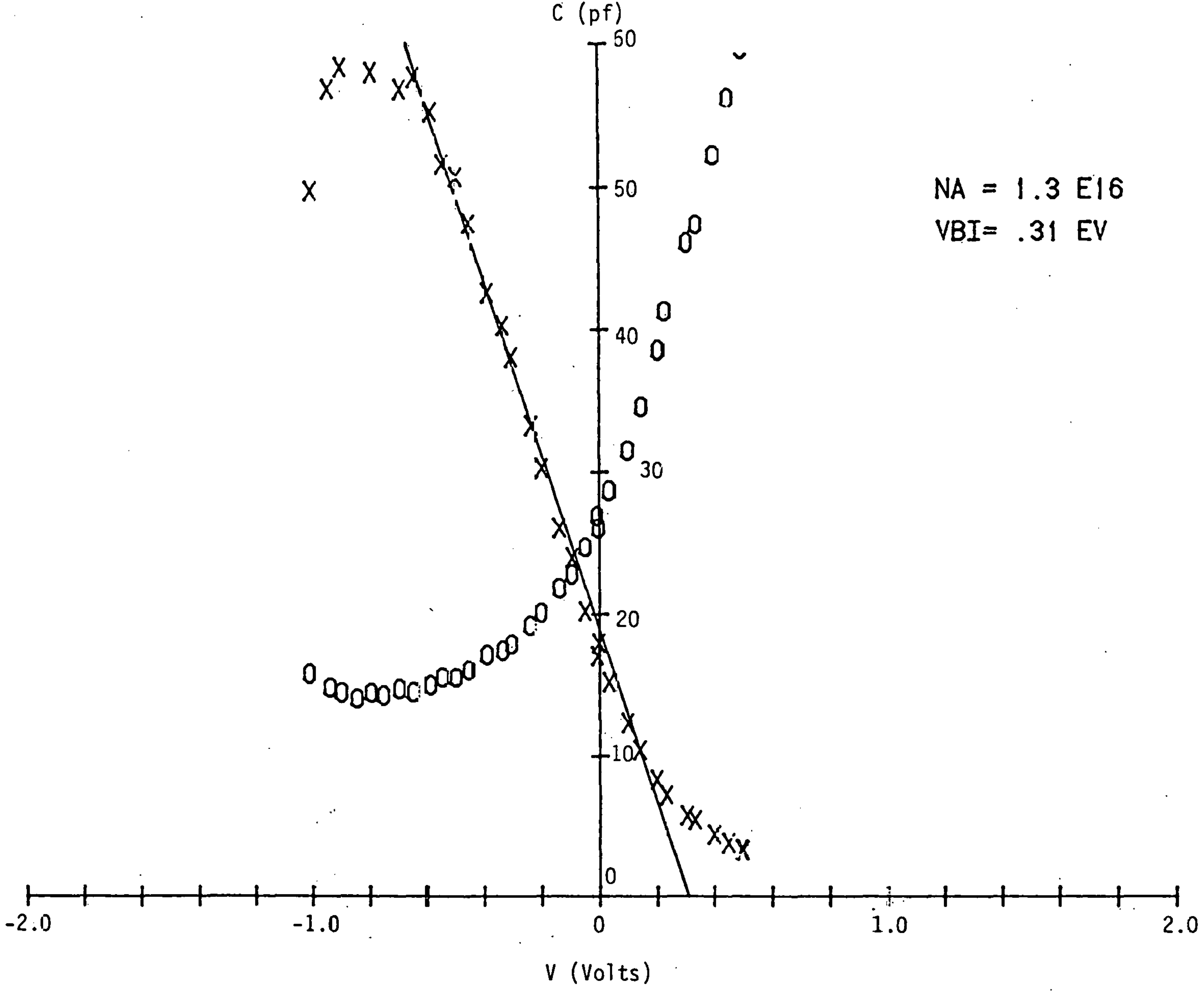

Fig. 4. C-V (O) and $1/C^2$-V (x) characteristics of $(CH)_x$:Mg Schottky barrier.

The results of these measurements are encouraging and must be placed in context. Schottky barriers formed in polycrystal conventional semiconductors (e.g., Si or GaAs) with a grain size equal to the fibrile diameter of the $(CH)_x$ (100-1000Å) would not exhibit rectification. In the coming quarter, we will repeat the measurements on both undoped and doped $(CH)_x$ using both opaque and semitransparent structures and carry out photo-measurements such as illuminated I-V and photoresponse.

II. Development of FET Structures

In the last quarterly report, the inapplicability of magnetic measurements (i.e., Hall effect) to polymers was discussed and the need to develop a JFET measurement was described. In the JFET measurement, the source and drain contacts are made to the polymer and the mobility and doping are independently determined from the pinch-off voltage and current, i.e., directly from transport measurement. At the end of the last quarter, the remaining problems were to obtain pin-hole free oxides and to apply the source and drain contacts without shorts to the base semiconductor.

During this quarter, a new mask set was developed which results in the structure shown in Fig. 5. Samples were fabricated on silicon base material with thermal oxides and were found to be electrically adequate for the JFET measurements. At the end of the quarter, a supply of samples was forwarded to Pennylsvania for polymer deposition and measurement. During the coming quarter, we will fabricate samples from both Si and GaAs and assist in the measurements as needed.

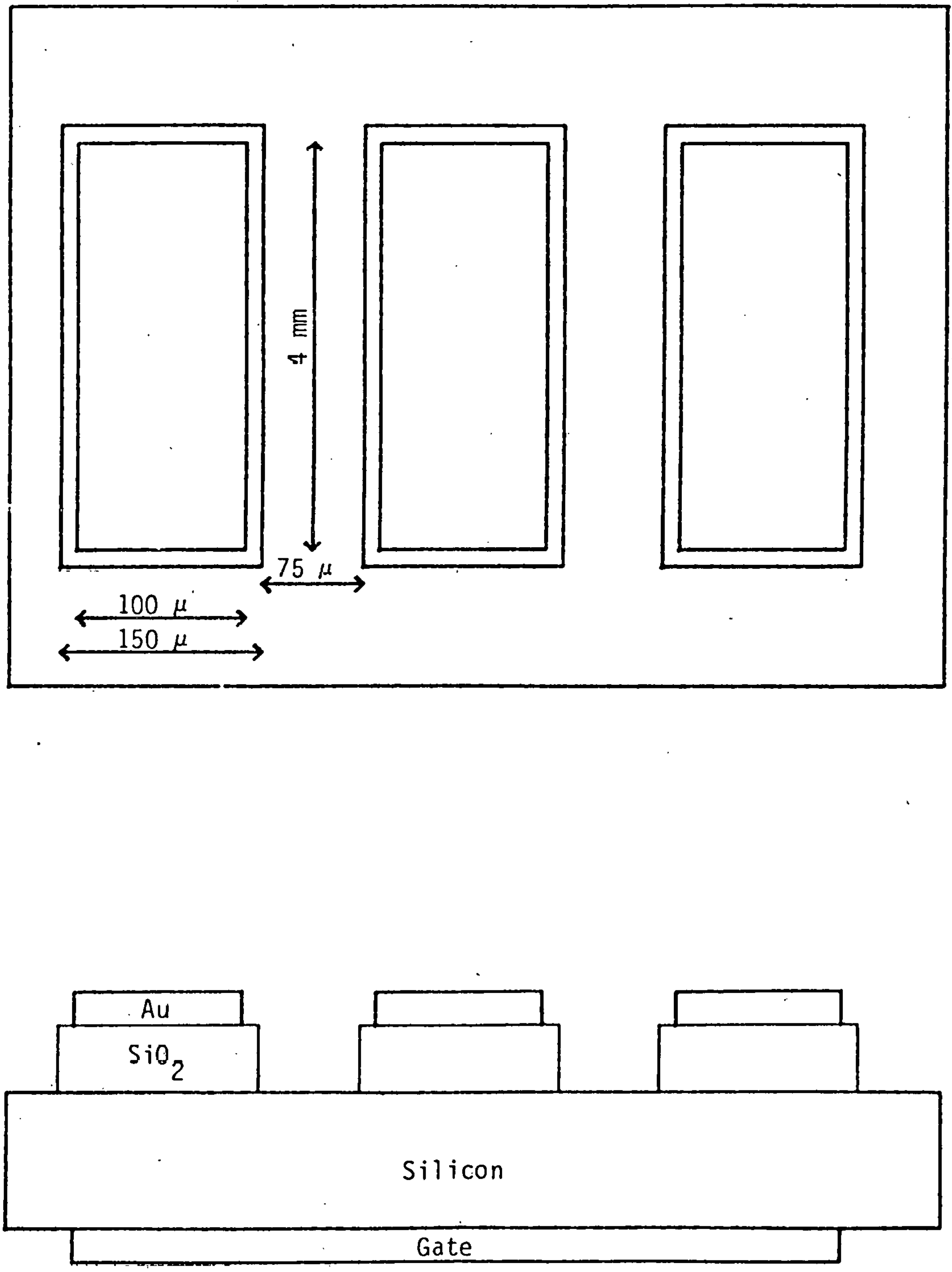

Fig. 5. JFET Structure.

☆U.S. GOVERNMENT PRINTING OFFICE: 1980-640-258/2299